



# CHARACTERIZATION OF COLD-FORMED STEEL FRAMED / WOOD-SHEATHED FLOOR AND ROOF DIAPHRAGM STRUCTURES

Violetta Nikolaidou<sup>(1)</sup>, Patrick Latreille<sup>(2)</sup>, Colin A. Rogers<sup>(3)</sup>, Dimitrios G. Lignos<sup>(4)</sup>

<sup>(1)</sup> PhD Candidate, McGill University, Department of Civil Engineering and Applied Mechanics, Montreal, Canada, [violetta.nikolaidou@mail.mcgill.ca](mailto:violetta.nikolaidou@mail.mcgill.ca),

<sup>(2)</sup> Master's Student, McGill University, Department of Civil Engineering and Applied Mechanics, Montreal, Canada, [patrick.latreille@mail.mcgill.ca](mailto:patrick.latreille@mail.mcgill.ca),

<sup>(3)</sup> Associate Professor, McGill University, Department of Civil Engineering and Applied Mechanics, Montreal, Canada, [colin.rogers@mcgill.ca](mailto:colin.rogers@mcgill.ca),

<sup>(4)</sup> Associate Professor, École Polytechnique Fédérale de Lausanne, School of Architecture, Civil & Environmental Engineering, Lausanne, Switzerland, [dimitrios.lignos@epfl.ch](mailto:dimitrios.lignos@epfl.ch)

## Abstract

The seismic in-plane response of cold-formed steel (CFS) framed diaphragm structures has not been the subject of extensive study. The information available specific to diaphragm design in the North American CFS design standard is based on limited experimental work and the extrapolation of design methods developed for the wood industry. Nonetheless, buildings having floor and roof diaphragms framed with thin steel joist members and wood sheathing panels are being constructed in North America. To address these shortcomings a test-based research project was carried out at McGill University. The objective was to provide characterization of typical CFS framed / wood-sheathed diaphragm response to in-plane lateral loading, in order to better understand the structural performance, and to provide full force vs. deformation hysteretic parameters for use in subsequent design method development and nonlinear response history analyses of CFS framed structures. This research was a complementary study to the CFS – NEES a project, which involved the dynamic testing of a full-scale two storey CFS framed building. The work detailed herein includes diaphragm test specimens that were based on the floor and roof configurations used in the CFS - NEES Building. The objective was to obtain information regarding the response to loading of the isolated diaphragm systems. The specimens were comprised of oriented strand board (OSB) sheathing screwed to CFS C-Channel joists. Eight 3.66 x 6.1m diaphragm configurations were tested under monotonic and reversed cyclic loading. Design predictions for the shear strength and stiffness of the diaphragm configurations are also included following the provisions of the AISI S213 & AISI S400 Standards.

*Keywords: in-plane loading; diaphragm; cold-formed steel; experimental program; shear response*

## 1. Introduction

Cold-formed steel (CFS) framed structures are widely used for both residential and commercial purposes due to their efficiency and cost effectiveness. The lateral force resisting system (LFRS) of these structures involves CFS framed diaphragms and shear walls, with the latter being the primary component. Although extensive experimental and numerical work has been realized for the lateral response of shear walls [2,3,4,5], little research exists on the diaphragm behaviour under in-plane loading and its contribution to the overall seismic response of the CFS structure. Moreover, the design provisions for CFS framed diaphragms for use in the US offered in the current seismic code provisions are based largely on experimental work on wood diaphragms and shear walls, while there is no seismic design procedure available for CFS framed diaphragms for use in Canada [1,6,7]. Therefore, the need to address these design deficiencies is evident in order to assist professional engineers in the construction of safer and more economical CFS structures.

A critical part of the design process is to ensure adequate shear capacity and stiffness for the diaphragm by means of designing suitable connections between the sheathing and the framing, as well as between the diaphragm and the vertical LFRS components [8]. Lum's analytical work [9] provided allowable design shear strength values for a limited number of CFS framed / plywood sheathed diaphragm configurations based on the methodology included in Tissell and Elliot [10] for wood framing. These design values are included in Table F2.4-1 of the AISI S400 Standard [1]. Moreover, a deflection equation for simply supported diaphragms (Eq. C-F2.4.3-1 [1]) proposed by Serrette and Chau [11] is available in AISI S400. Shear strength and stiffness values were also made available by the National Association of Home Builders Research Center [12], which carried out



four monotonic tests on CFS framed / oriented strand board (OSB) sheathed diaphragms and studied the individual sheathing to framing connection response.

A major research project involving the dynamic testing of CFS framed buildings, known as the CFS - NEES project, which involved a full-scale two storey CFS framed building tested on a shake table under earthquake loading, was conducted by researchers at Johns Hopkins University [13]. The main focus of this research program was the investigation of the overall seismic response of the CFS framed structure, with particular emphasis on the characterization of the isolated CFS framed - wood sheathed shear walls [13, 5]. Although the CFS – NEES project provided an insight into the global seismic response of CFS structures, more information was required regarding the isolated seismic performance of the diaphragm subsystem.

The experimental work presented herein focuses on the characterization of the behaviour of CFS framed / OSB sheathed roof and floor diaphragms under in-plane loading. The diaphragm specimens were tested in the Jamieson Structures Laboratory at McGill University and were based on the floor and roof configurations used in the CFS - NEES Building. A cantilever diaphragm test approach was followed for which the specimen dimensions were 3.66 m x 6.1 m. A self-reacting frame was initially designed and constructed as a test-setup in order to accommodate the diaphragm specimens. Four diaphragm configurations were selected, each of which was tested under in-plane monotonic and reversed cyclic loading, resulting in a total of eight test specimens. The CUREE (Consortium of Universities for Research in Earthquake Engineering) [14] reversed cyclic displacement controlled loading protocol was employed. In addition to describing the testing and test results, this paper contains a comparison between the measured test values and the calculated shear strength and deflection values following the AISI S400 Standard [1].

## 2. Diaphragm test program

### 2.1 Test setup

A self-reacting braced frame was designed for the purposes of the experimental program presented in this paper (Fig. 1). W-shape sections were used for the main beams comprising the frame, while double angle sections were used for the bracing. The three short beams and the braces were pin-connected while the two long beams were continuous. The design of the frame members and connections was based on the CSA S16 design standard [15] and on the results of analyses using the SAP2000 commercial software [16], where a 2D model was employed. The design load was based on the actuator's ultimate tensile capacity (450KN) and on previous shear wall and diaphragm testing described in the literature, which suggested that the maximum load would not exceed 200KN [2, 3, 4, 5, 12]. The main objective in the design of the test setup was for the frame to remain elastic during the test and to have adequate stiffness to exhibit the minimum possible deformation. A roller support system was employed in order for a W-shape distribution beam to be attached to the actuator and the specimen. The beam in question was able to move laterally distributing the force to the specimen following the movement of the actuator. The specimen was fixed at the other side of the frame by being bolted to built-up I shape sections, which were bolted to the frame. Since the diaphragm specimen dimensions were 3.66 x 6.1m the frame dimensions were chosen to be 4.5 x 6.5m, taking into account the space limitations of the Jamieson Structures Laboratory. It should be noted that, although all the in-plane forces were expected to be taken by the frame (self-reacting), a maximum lateral load of 50KN was considered for the 38mm anchor rods, connecting the frame to the strong floor as a safety measure. Four roller supports were implemented in the analysis model, restricting the movement of the frame in the y direction, while allowing it to move laterally (x direction) in order to obtain an approximation of the forces to be expected during the test. A roller support was also placed in the actuator location restricting the x direction in order for the reaction force applied from the actuator to the frame to be simulated. The fixed connection was braced against potential rotation during the test using single angle sections, as shown in Fig. 1. It is worth mentioning that during testing the test setup fulfilled its purpose as a self-reacting frame. Based on the instrumentation set in place as explained in Section 2.3, the in-plane forces were taken by the frame and not the anchor rods, and there was zero displacement observed by the frame throughout the testing process.

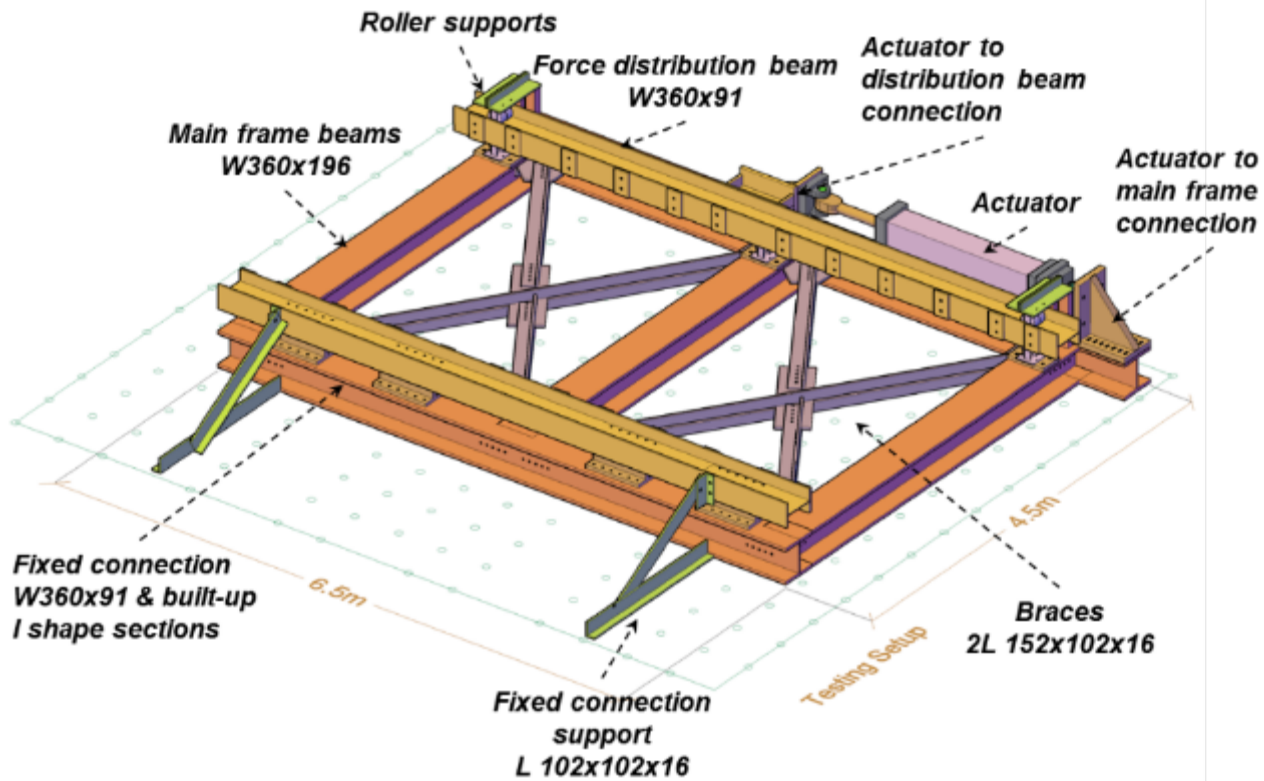


Fig. 1 – CFS diaphragm test setup

## 2.2 Diaphragm configurations

As mentioned in Section 1, the diaphragms tested were based on two basic configurations, the floor and roof diaphragms of the CFS - NEES Building, which varied in steel thickness (1.37 mm vs. 2.46 mm) and OSB panel thickness (11.1mm vs. 18.2mm with tongue and groove edges). After the two basic configurations were tested, full panel blocking was added to the roof configuration, where the full perimeter of each OSB panel was fastened to the underlying steel framing, and a larger sheathing screw size (#12) was used in the floor configuration to investigate the effect of these two parameters on the shear strength and stiffness of the diaphragm. Thus, this experimental program included a total of four configurations and eight tests, since each configuration was tested under monotonic and reversed cyclic loading. Two additional monotonic tests were realized for the bare CFS framing without the sheathing in order for its contribution to be accounted for separately. Fig. 2 contains an illustration of one of the diaphragm configurations (unblocked). Table 1 includes the characteristics for the two basic floor and roof diaphragm configurations. ASTM A653 Grade 50 (345 MPa) steel was used for the fabrication of the joists and tracks. It should be noted that the double joist section illustrated in Fig. 2 was placed in an effort to include the stiffening effect of a wall attached to the diaphragm. Moreover, the ledger framing used in the CFS - NEES building included a 152.4mm extension of the sheathing inside the walls. For purposes of consistency a 152 mm extension of the wood panels was allowed at the fixed connection location, as shown in Fig. 3 leading to an out-to-out dimension of the CFS frame of 3505mm. Fig. 3 demonstrates one of the specimens attached to the test setup. Table 2 contains the nomenclature for the test specimens.

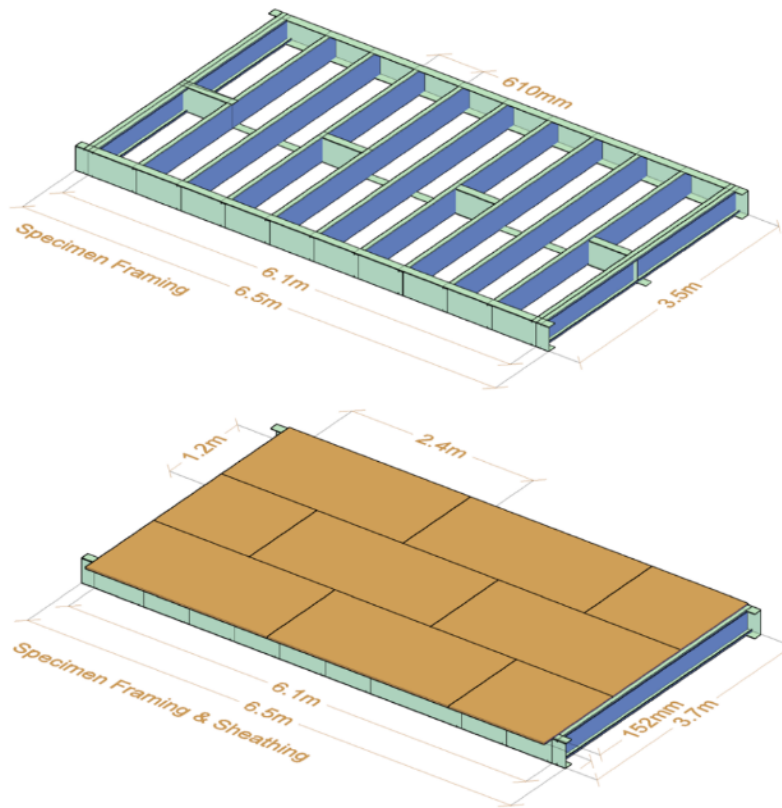


Fig. 2 – CFS framing and wood panel sheathing illustration

Table 1 – Floor and roof diaphragm configurations

Configuration Roof (Gr. 50, 345MPa)	Section (mm)	Length (mm)
<b>Joists</b>	305S51-137M	3505
<b>Rim Joists</b>	305T51-173M	6480
<b>Web Stiffeners</b>	L 38x38x1.37	250
<b>Joist bracing</b>	305S41-137M	560
<b>Joist bracing connectors</b>	L 38x102x1.37	250
<b>Straps</b>	38x1.37	6300
<b>#8 sheathing self-drilling (152/305mm spacing)</b>	-	50
<b>#10 steel-to-steel flat head self-drilling</b>	-	20
<b>#10 steel-to-steel Hex Head Cap self-drilling</b>	-	25
<b>OSB panels (24/16 rated)</b>	2400x1200x 11	-

Table 1 (Continued) – Floor and roof diaphragm configurations

Configuration Floor (Gr. 50, 345MPa)	Section (mm)	Length (mm)
<b>Joists</b>	350S64-246M	3505
<b>Rim Joists</b>	350T64-246M	6480
<b>Web Stiffeners</b>	L 38x38x1.37	280
<b>Joist bracing</b>	305S51-137M	550
<b>Joist bracing connectors</b>	L 38x102x1.37	250
<b>Straps</b>	38x1.37	6300
<b>#10 sheathing self-drilling (152/305mm spacing)</b>	-	44
<b>#10 steel-to-steel flat head self-drilling</b>	-	20
<b>#10 steel-to-steel Hex Head Cap self-drilling</b>	-	25
<b>OSB panels (48/24 rated)</b>	2400x1200x 18	-



Fig. 3 – Roof specimen (unblocked) attached to test setup

Table 2 – Specimens nomenclature

Specimen	Description
<b>1-RF-M</b>	Roof Bare Steel Frame Monotonic
<b>2-FF-M</b>	Floor Bare Steel Frame Monotonic
<b>3-RU-M</b>	Roof Unblocked Monotonic
<b>4-RU-C</b>	Roof Unblocked Cyclic
<b>5-F#10-M</b>	Floor #10 Screws Monotonic
<b>6-F#10-C</b>	Floor #10 Screws Cyclic
<b>7-RB-M</b>	Roof Blocked Monotonic
<b>8-RB-C</b>	Roof Blocked Cyclic

Table 2 (Continued) – Specimens nomenclature

Specimen	Description
9-F#12-M	Floor #12 Screws Monotonic
10-F#12-C	Floor #12 Screws Cyclic

### 2.3 Instrumentation

Extensive instrumentation was employed in order to study the lateral response of the diaphragm configurations during testing. Four string potentiometers ( $\pm 254$  mm & 508 mm stroke) were required to capture the lateral displacement and overall shear deformation of each diaphragm, and twelve linear variable differential transformers (LVDTs  $\pm 15$  mm stroke) to measure the local in-plane displacement. Strain gauges were also attached to the end joists (chords) in an effort to obtain the axial force of the chords. It should be noted that the information gained from the strain gauges with respect to the axial force of the chords, although reasonable in value, could not be relied upon given that the stress distribution in the CFS joists was not uniform. The capacity curve for each diaphragm configuration was obtained using the data provided by the string potentiometer and the load cell of the actuator. Figures 4a and b indicate the locations of the instruments. The measurement instruments were connected to Vishay Model 5100B scanners that were used to record data using the Vishay System 5000 StrainSmart software.

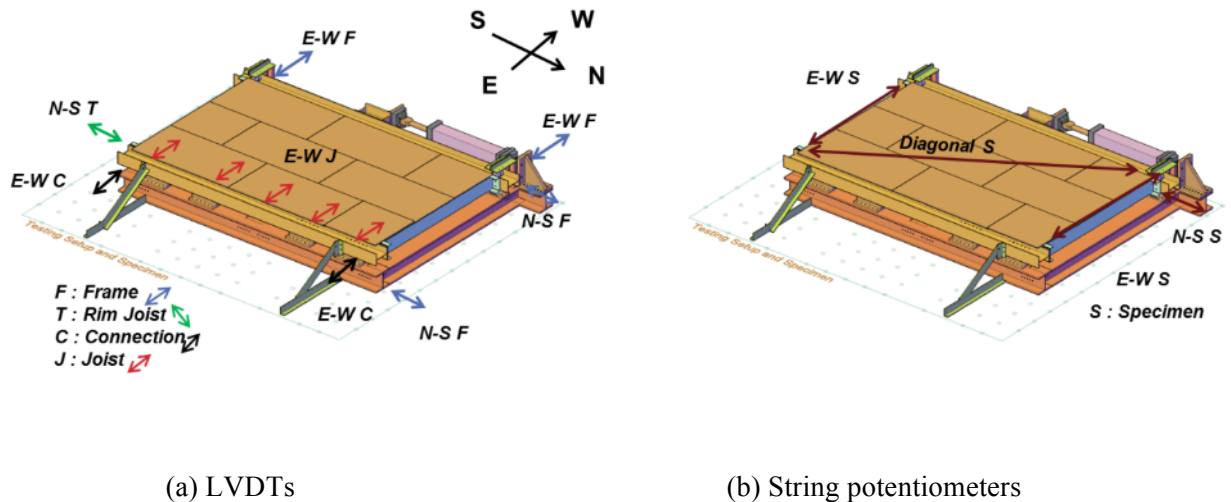


Fig. 4 – Instrumentation

### 2.4 Material properties

Following the ASTM 370 Standard [17] tensile coupon specimens with 50 mm gauge length were extracted from the CFS sections (joists and rim joists) and tested. The different steel thicknesses were considered with three coupons tested for each case (roof rim joist, roof joist, floor rim joist, floor joist). Strain gauges were placed to obtain an accurate value of the Young's modulus while an extensometer with a gauge length of 50 mm was attached to the middle of the specimen in order to measure the elongation. A visual method was also implemented where the coupons were punch-marked at 50.8 mm gauge distance in the middle of the specimen before the test and then the distance between these two points was measured again after the test had finished. The nominal yield stress of steel was 345MPa. The specimens showed sharp yielding behaviour. Table 3 summarises the results from the tensile coupon tests. Increased yield stress values were expected due to the fabrication process of cold-formed steel. Moisture content measurements were also conducted on the OSB panels. Three round specimens per panel (76.2mm) were extracted from selected panels immediately after testing and their weight was measured. The secondary oven-drying method of ASTM D4442 Standard [18]



(Method B) was employed, where the specimens were placed for 24 hours in a constant oven temperature of 103°C in order for the oven - dry mass to be obtained. Low moisture content in the range of 4% to 5% was obtained, as expected due to the fabrication process of the OSB panels.

Table 3 – Tensile properties of steel

Specimens	E (MPa)	F <sub>y</sub> (MPa)	ε <sub>y</sub> (mm/mm)	F <sub>u</sub> (MPa)	ε <sub>u</sub> (mm/mm)	F <sub>u</sub> /F <sub>y</sub>	Elongation (%)	No.
<b>RJ - Roof</b>	188595	387	0.0040	466	0.1717	1.20	27.5	3
<b>RJ - Floor</b>	224149	398	0.0028	474	0.1822	1.19	31.8	3
<b>J - Roof</b>	189049	391	0.0037	471	0.1959	1.20	28.7	3
<b>J - Floor</b>	210854	394	0.0036	462	0.1695	1.17	29.3	1
<b>J - Roof B</b>	200568	385	0.0015	466	0.0673	1.21	14.8	3
<b>J - Floor #12</b>	202097	410	0.0018	477	0.0858	1.16	14.6	3

Table 3 Notes:

1. In the blocked roof diaphragm and the floor diaphragm using #12 sheathing screws new steel joists were ordered; thus, extra coupons were provided and tested for these steel sections (J - Roof B, J - Floor #12).
2. RJ = Rim Joist, J = Joist.

## 2.5 Loading protocol

The CUREE displacement controlled loading protocol for ordinary ground motions [14] was followed for the reversed cyclic loading tests to represent an earthquake excitation with a probability of exceedance of 10 % in 50 years. The protocol incorporates a number of smaller cyclic excitations prior to the larger deformation amplitudes; thus, considering the effect of cumulative damage on the specimen. The protocol required first a monotonic test to be conducted for each of the diaphragm configurations in order for a reference displacement to be obtained, which was subsequently multiplied by a 0.6 reduction factor to account for the earlier deterioration in the specimen strength expected under cyclic loading. A displacement rate of 2.5mm/min for the roof and 5mm/min for the floor configuration was applied during the monotonic loading, while the cyclic loading followed a displacement rate that started with 15mm/min and increased to 60mm/min after approximately 60mm of displacement for both the roof and floor configurations.

## 3. Diaphragm test results

### 3.1 Test results

The bare steel frame was first tested under monotonic loading to a maximum displacement of 45 mm in order for the specimen to remain in the elastic range. The shear strength and stiffness contribution of the bare steel frame was found to be negligible. Subsequently, the results for specimen 3-RU-M, 4-RU-C, 5-F #10-M and 6-F #10-C were carried out. Fig. 5 and 6 provide the shear response vs. rotation curves for all the diaphragm configurations tested in the form of a comparison between blocked vs unblocked roof diaphragm configurations (7-RB-M, 8-RB-C vs. 3-RU-M,4-RUC) and the floor configuration with #12 sheathing screws vs the #10 ones (9-F#12-M, 10-F#12-C vs. 5-F#10-M,6-F#10-C), respectively.

Fig. 7 and 8 demonstrate the damage inflicted on the diaphragm during testing for specimens 3-RU-M, 4-RU-C and 5-F#10-M, 6-F#10-C, respectively. The damage for specimens 3 and 4 (3-RU-M,4-RU-C) was characterized by screws tearing out or pulling through the wood after wood bearing had occurred, which these failures concentrated in the middle row of the panels where fewer screws were used (unblocked diaphragm, 304mm). Tilting of the screws was present, which is a desired deformation mode (energy dissipation). Lift-off of panels in these intermediate locations was observed as illustrated in Fig. 7.

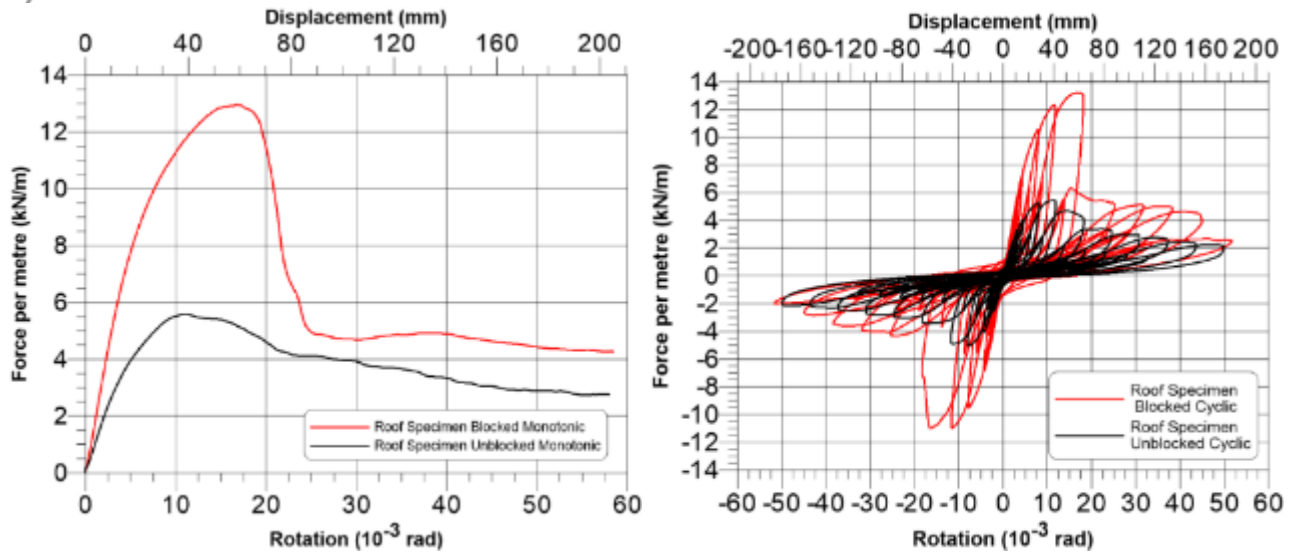


Fig. 5 – Force vs. deformation response for specimens 3-RU-M, 4-RU-C, 7-RB-M & 7-RB-C

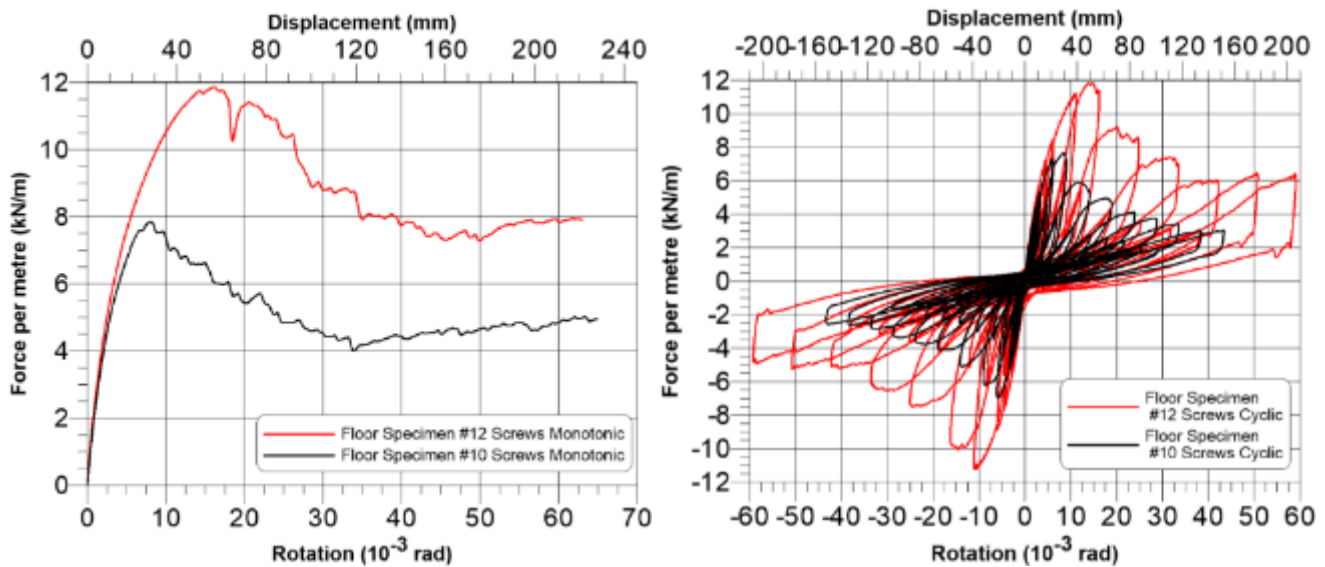


Fig. 6 – Force vs. deformation response for specimens 5-F#10-M, 6-F#10-C, 9-F#12-M & 10-F#12-C

The response curve for the floor diaphragm configuration with the #10 screws (5-F#10-M, 6-F#10-C, Fig. 6) shows a steeper decline of the shear strength compared to the roof unblocked configuration (3-RU-M, 4-RUC, Fig. 6). During testing, it became evident that the #10 sheathing screws were not adequate for the sheathing and steel thickness of the diaphragm, as they were primarily failing in shear or remaining vertical while the wood sheathing was tearing out. Shear failure is a brittle failure mode which resulted in the quick loss of strength after the maximum load was reached. Moreover, an increase in shear strength during the monotonic test was observed after approximately 35mrad of rotation (Fig. 6) while the final excursions of the cyclic test showed that the load was being maintained at a certain level. This effect was attributed to the fact that a contact/bearing action was taking place between the edges of the OSB panels in the intermediate locations after most of the screws had failed. The tongue & groove (T&G) characteristic of the OSB panels for the floor diaphragm configuration aided in the development of this additional resistance since lift-off of panels in this case was prevented. Fig. 8 illustrates the failure mode and contact effect for the 5-F#10-M and 6-F#10-C specimens described herein.



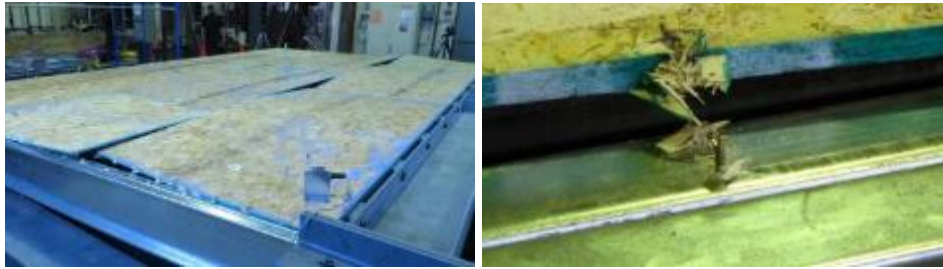


Fig. 7 – Deformation for the roof unblocked diaphragm configurations, 3-RU-M & 4-RU-C



Fig. 8 – Deformation for floor diaphragm configurations with #10 screws, 5-F#10-M & 6-F#10-C

During testing of the blocked roof diaphragm configuration (7-RB-M, 8-RB-C) failure was concentrated to the wood panels near the fixed connection location, as shown in Fig. 9. The fact was that the edge wood panels in that location extended 152 mm into the connection, as explained in Section 2.2. Effectively, a shorter width panel was connected to the steel framing in that location; thus, fewer screws were used. The screws were tilting, shearing or pulling through the OSB primarily in that location. Ultimately, the sheathing connections in these edge panels failed resulting in a transfer of force through the underlying steel framing by means of bending action (cantilever moment frame action of the steel framing in that location since there was no more diaphragm action, Fig. 9). This bending action of the steel framing justifies the constant level of the shear force after approximately 90 mm indicated in the response curve in Fig. 5.



Fig. 9 – Bending action of steel framing, specimen 7-RB-M & 8-RB-C

The larger screw size (#12 vs. #10) for the floor configuration (9-F#12-M & 10-F#12-C) resulted in an effective redistribution of forces during testing. All sheathing screws were contributing with shear and tensile forces leading to screw tilting before shearing or pulling out of the steel. Several joist flanges were extensively distorted due to the applied uplift forces of the panels. Wood panel edge contact action in the intermediate panel locations was again present. Tables 4 summarises the corresponding data for all the specimens from the monotonic tests. Specimens 5 and 6 (5-F#10-M, 6-F#10-C, floor) exhibited higher shear strength compared with specimens 3 and 4 (3-RU-M, 4-RU-C, roof). However, specimens 5 and 6 experienced a more rapid post-peak decrease in strength, as shown in Figs. 5 and 6. Based on Table 4, the blocked roof diaphragm configuration (7-RB-M, 8-RB-C) exhibited the highest shear strength and stiffness. As, shown in Fig. 5 the addition of blocking had a profound effect on the diaphragm's response to in-plane loading, which led to a 130% increase in shear strength



and a 70% increase in shear stiffness. The effect of the larger screw size led also to an increase of shear strength of 50%; however, based on Fig. 6 the shape of the overall force vs. deformation response of the diaphragm was not greatly influenced by the #12 screw size.

Table 4 – General results from the monotonic tests

Specimens	$S_u$ (KN/m)	$\Delta_{net,o.4u}$ (mm)	$\Delta_{net,u}$ (mm)	$\theta_{net,u}$ (rad x 10 <sup>-3</sup> )	Rigidity, K (KN/mm)
<b>3-RU-M</b>	5.6	9	41.5	11.8	1.53
<b>5-F#10-M</b>	7.9	6.1	30	8.6	3.15
<b>7-RB-M</b>	13	12	62.1	17.7	2.64
<b>9-F#12-M</b>	11.8	9.4	60.7	17.3	3.07

## 4. Design predictions

### 4.1 Deflection design values

Deflection design values for the diaphragm test specimens were obtained using Eq. E1.4.1.4-1 [1] which refers to the deflection of blocked CFS framed/wood sheathed shear walls in the AISI S400 Standard. Although a diaphragm related deflection equation is also available (Eq. C-F2.4.3-1 [1]), the shear wall deflection equation (Eq. 1 in this paper) was deemed more appropriate because of the cantilever support condition utilised in the tests.

$$\delta = \frac{2vh^3}{3E_s A_c b} + \frac{\omega_1 \omega_2 v h}{\rho G t_{sheathing}} + \omega_1^4 \omega_2 \omega_3 \omega_4 \left(\frac{v}{\beta}\right)^2 + \frac{h}{b} \delta_v \quad (1)$$

- Ac = Gross cross-sectional area of chord member (mm<sup>2</sup>)
- b = Width of the shear wall (mm)
- Es = Modulus of elasticity of steel 203,000 MPa
- G = Shear modulus of sheathing material, G = 1317 MPa
- H = Wall height (mm)
- S = Maximum fastener spacing at panel edges (mm)
- t<sub>sheathing</sub> = Nominal panel thickness (mm)
- t<sub>stud</sub> = Nominal framing thickness (mm)
- v = Shear demand (V/b), (N/mm)
- V = Total in-plane load applied to the diaphragm (N)
- β = 2.35 for plywood and 1.91 for OSB for SI units (N/mm<sup>1.5</sup>)
- δ = Calculated deflection (mm)
- δ<sub>v</sub> = Vertical deformation of anchorage / attachment details (mm)
- ρ = 1.85 for plywood and 1.05 for OSB
- ω<sub>1</sub> = s/152.4 (for s in mm)
- ω<sub>2</sub> = 0.838/t<sub>stud</sub> (for t<sub>stud</sub> in mm)
- ω<sub>3</sub> = √((h/b)/2)
- ω<sub>4</sub> = 1 for wood with structural panels

In addition, it was observed that focusing on the elastic range of the force vs. deformation response would reduce the error between calculated and observed deflection values. To this end, the elastic stiffness, δ<sub>ELASTIC</sub>, of each test specimen was calculated based on the 40% of shear demand level. The δ<sub>ELASTIC</sub> is the maximum deflection assuming an elastic system using the in-plane lateral elastic stiffness, K<sub>e</sub>. The results of this process are summarised in Table 5. For the unblocked specimens an amplification factor should be implemented since Eq. 2 refers only to blocked systems. The 2.5 factor suggested for the diaphragm deflection equation (Eq. C-F2.4.3-1 AISI S400 [1]) is based on experimental data of simply supported wood diaphragm configurations [8];



thus, its application is questionable for the data presented herein. Moreover, it should be noted that Eq. 2 in this report is based on experimental work of 1220 x 2440 mm shear walls [11]. The behaviour of a single panel fully blocked shear wall is characterized by gradual yielding, which does not comply with the sharp drop of strength exhibited by the diaphragm configurations after the peak load was reached, as described in Section 3 of this paper.

Table 5 – Design deflection values using Eq. 2 and comparison with  $\delta_{ELASTIC}$

Diaphragm Specimens	3-RB-M & 4-RB-C	5-F#10-M & 6-F#10-C	7-RB-M & 8-RB-C	9-F#12-M & 10-F#12-C
$\delta_{Calculated}$ (mm)	10.0	8.35	29.4	14.4
$\delta_{ELASTIC}$ (mm)	22.4	13.2	29.5	23.5
% Error	55.4	36.7	0.0	38.7

#### 4.2 Shear design values

Table F2.4-1 is included in the new AISI S400 Standard [1] providing design shear strength values for a limited number of diaphragm configurations with CFS framing and plywood sheathing [9]. Table 6 lists the design shear strength values ( $V_{design}$ ) to be considered for each diaphragm test configuration based on the information of Table F2.4-1 and the measured shear resistance values ( $V_{test}$ ). Table F2.4-1 refers only to plywood sheathing and does not account for the effect of the sheathing screw size. These limitations do not allow for design predictions to be made corresponding to the specific tested diaphragm specimens; however, these are the only design values available at present in the AISI S400 Standard [1].

Table 6 – Shear resistance design values using Table F2.4-1 of AISI S400 [1]

Diaphragm Specimens	3-RB-M & 4-RB-C	5-F#10-M & 6-F#10-C	7-RB-M & 8-RB-C	9-F#12-M & 10-F#12-C
$V_{design}$ (KN/m)	7.37	8.10	11.10	8.10
$V_{test}$ (KN/m)	5.6	7.9	13	11.8

## 5. Conclusions

This paper describes the results obtained from an experimental program focused on the characterisation of in-plane force vs. deformation response of CFS framed OSB sheathed diaphragms under monotonic and reversed cyclic loading. The program consisted of four diaphragm configurations and a total of ten tests, for which parameters such as steel sections, OSB thickness, screw size and blocking were varied. Blocking was able to increase the shear strength and stiffness of the diaphragm and had a direct impact on its response to load. The increase of screw size led to an increase in shear strength of the diaphragm and a different sheathing-to-framing screw connection behaviour; however, the shape of the overall force vs. deformation response remained the same. The bare steel frame contribution to shear strength and stiffness was found to be negligible. Moreover, the limited information available in the AISI S400 Standard [1] did not allow for reliable design shear strength values to be obtained. In addition, using the shear wall deflection equation (Eq. 1 in this paper) of the AISI S400 Standard [1] led to a meaningful comparison between the calculated and observed data only by assuming elastic response of the diaphragm. The work presented herein is part of an extensive experimental program aiming to shed light on the complicated nature of diaphragm subsystems.



## 6. Acknowledgements

The authors would like to thank the American Iron and Steel Institute (AISI) for financially supporting this research project. Additional support was obtained from the Canadian Sheet Steel Building Institute (CSSBI) and the Natural Sciences and Engineering Research Council of Canada (NSERC). A special thank you is also extended to Bailey Metal Products Ltd., Simpson Strong-Tie Co. Inc., Ontario Tools and Fasteners Ltd, ArcelorMittal and Constructions Proco Inc. for the materials and tools that have been provided.

## 7. References

- [1] AISI S400 (2015): *North American Standard for Seismic Design of Cold-Formed Steel Structural Systems*. American Iron and Steel Institute, Washington, USA.
- [2] Branston, A.E. (2004): Development of a design methodology for steel frame / wood panel shear walls. *M.Eng. Thesis*, Department of Civil Engineering and Applied Mechanics, McGill University, Montreal, Qc, Canada.
- [3] Boudreault, F.A. (2005): Seismic analysis of steel frame / wood panel shear walls. *M.Eng. Thesis*, Department of Civil Engineering and Applied Mechanics, McGill University, Montreal, Qc, Canada.
- [4] Blais, C. (2006): Testing and analysis of light gauge steel frame / 9mm OSB wood panel shear walls. *M.Eng. Thesis*, Department of Civil Engineering & Applied Mechanics, McGill University, Montreal, QC, Canada.
- [5] Liu, P., Peterman, K.D., Yu, C., Schafer, B.W. (2012): Cold-formed steel shear walls in ledger-framed buildings. *Annual Stability Conference, Structural Stability Research Council*, April 2012, Grapevine, Texas, USA.
- [6] NRCC (2010): *National Building Code of Canada 2010, 13th Edition*. National Research Council of Canada. Ottawa, ON, Canada.
- [7] CSA S136-07 (2007): *North American Specification for the Design of Cold-Formed Steel Structural Members*. Canadian Standards Association, Mississauga, ON, Canada.
- [8] APA (2007): *Diaphragms and Shear Walls*. The Engineered Wood Association. Design/Construction Guide Form No. L350A.
- [9] LGSEA (1998): Lateral load resisting elements: Diaphragm design values. *Tech Note 558b-1*, Light Gauge Steel Engineers Association, Washington, DC, 1998.
- [10] Tissell, J. R. and Elliot, J. R. (2004): Plywood diaphragms. *Research Report 138*, American Plywood Association (APA), Tacoma, Washington, September 1993.
- [11] Serrette, R.L., and Chau, K. (2003): Estimating the response of cold-formed steel-frame shear walls. Santa Clara University. Santa Clara. CA
- [12] NAHB Research center (1999): Innovative residential floor construction: Horizontal diaphragm values for cold-formed steel framing. *U.S. Department of Housing and Urban Development*.
- [13] Peterman, K.D. (2014): Behaviour of full-scale cold-formed steel buildings under seismic excitations". *PhD Thesis*, Johns Hopkins University, Baltimore, Maryland.
- [14] Krawinkler, H., Parisi, F., Ibarra, L., Ayoub, A., Medina, R. (2000): Development of a testing protocol for wood frame structures. *Report W-02 covering Task 1.3.2*, CUREE/Caltech Woodframe Project. Consortium of Universities for Research in Earthquake Engineering (CUREE). Richmond, CA, USA.
- [15] CAN/CSA S16 (2014): *Design of steel structures*. Canadian Standards Association. Ontario, Canada.
- [16] CSI, SAP2000 V.14 (2009): *Linear and Non-linear Static and Dynamic Analysis and Design of Three-Dimensional Structures Basic Analysis Reference Manual*. Computers and Structures, Inc., Berkeley, California, USA.
- [17] ASTM A370 (2007a): *Standard Test Methods and Definitions for Mechanical Testing of Steel Products*. American Society for Testing and Materials, West Conshohocken, PA.
- [18] ASTM D4442 (2007): *Standard Test Methods for Direct Moisture Content Measurement of Wood and Wood Base Materials*. American Society for Testing and Materials, West Conshohocken, PA.